Bird Strike Modeling Using a New Woven Glass Failure Model

Lorenzo Iannucci and Mauricio Donadon
Department of Aeronautics
Imperial College London
South Kensington, London SW7 2AZ, U.K

Abstract

The bird strike impact problem is an increasing menace to the composite aerospace designer, especially since more aerospace components are being manufactured from composite materials. The LS-DYNA FE code is often used to model such an event as it can accurately represent the bird material behaviour and the contact between the bird and the structure. However, numerical simulations are usually accompanied by a parallel testing programme to validate the numerical simulations for some of these impact scenarios

.

The present paper described the implementation of an improved damage mechanics based material model to simulate the progressive failure of woven glass composites. A series of bird strike impacts on flat panels fabricated from low cost woven glass composite materials are used to validate the material model for practical composite component applications. The panels are modelled with shell elements only. The new material model can capture the strain rate enhancement to strength and strain observed for woven glass materials using a damage lag concept.

A hydrodynamic model for the bird, based on 90% water and 10% air, is used to represent the behaviour of the bird for all impact scenarios considered. The bird is heterogeneous in nature, however, a uniform material behaviour is assumed with a geometry based on a 2:1 length: diameter ratio with a cylindrical body and spherical end caps using mesh less Smooth Particle Hydrodynamic (SPH) techniques. Appropriate contact definitions are used between the bird and the composite panel. The simulations results are compared to experimental results and conclusions drawn.

Introduction

The rapid increase in the use of advanced composite materials in the design of aircraft, helicopters, boats, cars, etc. requires a detailed understanding of the behaviour of the composite component or structure to a wide range of potential external loadings, some of which may be severe. In particular in the aerospace industry, impact damage in laminated composite materials continues to be a major cause of concern. Typically impact damage can be generated from low velocity tool drop or runway debris, to high velocity impacts from birds or ballistic damage from missiles or shell fragments.

The fabrication, test and certification of these composite components and structures can be very expensive. However, advanced simulations will never eliminate the need for these expensive impact tests. In practise, they will require more detailed experimental tests to validate the advanced algorithms used within the Finite Element (FE) formulation. The major advantage of FE modeling is that they can study the effects of new and different structural and material concepts, without an extensive fabrication and testing programme.

In the current paper an updated woven glass material failure model is presented and used in a series of bird strike simulations. The bird is modelled using Smooth Particle Hydrodynamics (SPH) with the existing contact logic within the LS-DYNA code.

Bird Modeling

State-of-the-art explicit FE codes, such a LLNL DYNA3D or LS-DYNA, encompass a large number of material models which can simulate a wide range of physical behaviour. In the present simulations a hydrodynamic model is used to represent the behaviour of the bird for all impact scenarios considered.

Extensive databases of bird modeling strategies exist. A summary of these strategies are presented in the GARTEUR AG23 final report [1]. Based on these previous works the bird is model using 90% by volume of water with remainder of air. The model should have a length to breadth ratio of 2 and should consist of a cylindrical type structure with rounded ends. Figure 1 illustrates the recommended 1.82 kg (4lbs) bird geometry. The Equation of State (EOS) used for the bird is shown in Figure 2. The small percentage air (10%) dramatically affects the compressibility at low pressures, and hence must be included.

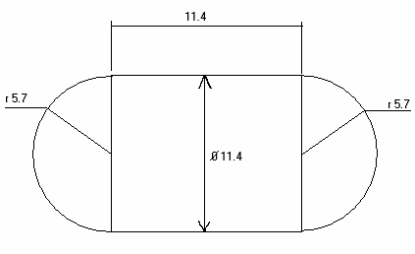

Figure 1: Bird Model Geometry (all dimensions are in cm) [1]

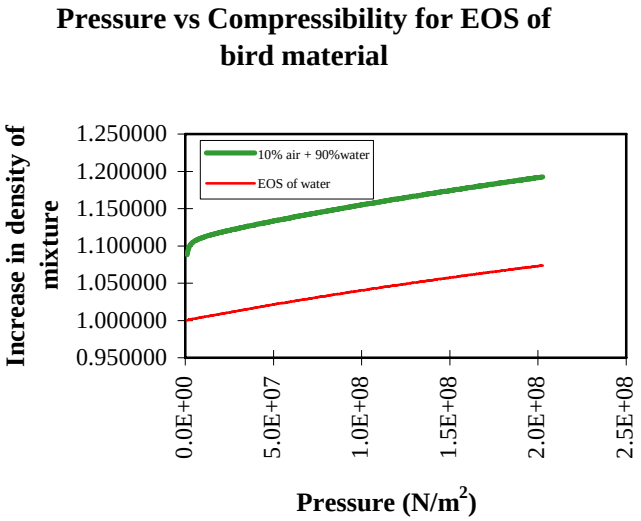

Figure 2: Equation of State for bird material in relation to the EOS of water [1]

The initial bird simulations [1, 2] were based on a pure Lagrangian FE formulation and have shown very good agreement with experimentally derived force-time and pressure-time history data.

Figures 3a to 3d shows the deformation of the bird mesh when impacting the rigid target. The figures clearly illustrate the Lagrangian bird flowing over the rigid surface. Also, the peak Hugoniot pressure occurs at approximately 35μsec into the impact event. Hence the percentage

of water and air within the bird EOS are critical in determining the peak Hugoniot pressures. Hugoniot pressures calculated with LS-DYNA using the fluid material model are shown to occur within the scatter of experimentally measured values.

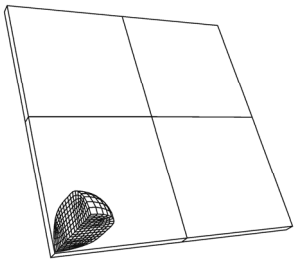

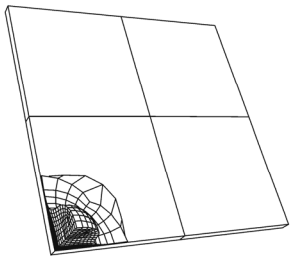

Figure 3a. Rigid wall bird strike impact, 250m/s, 1kg (time = 0μsec)

Figure 3b. Rigid wall bird strike impact, 250m/s, 1kg (time = 200μsec)

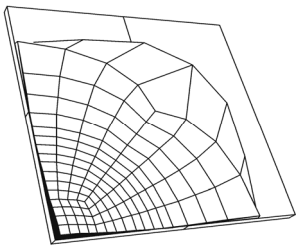

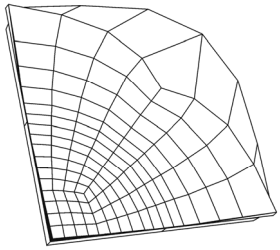

Figure 3c. Rigid wall bird strike impact, 250m/s, 1kg (time = 600μsec)

Figure 3d. Rigid wall bird strike impact, 250m/s, 1kg (time = 800μsec)

The numerically calculated pressure-time plot for a 1 kg impact at 250m/s is shown in Figure 4. The Hugoniot pressure was determined to be 300MPa and the Stagnation pressure was 30MPa, both are within the experimental scatter given in Barber et al [3].

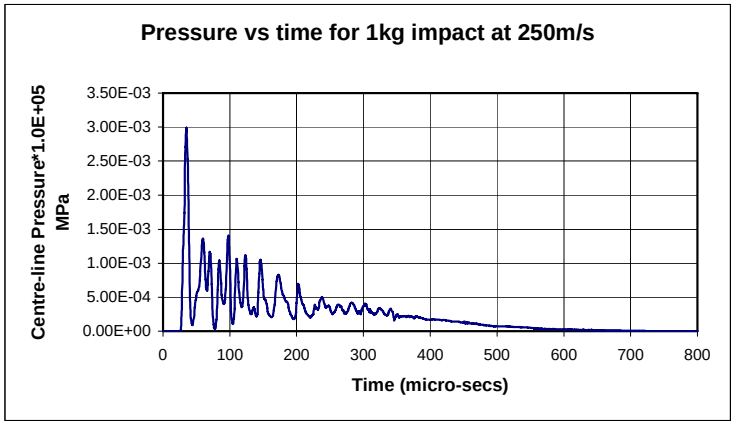

Figure 4. Pressure (x10^5MPa) vs. time (μsec) history for centre-line element of bird 250m/s: coarse Lagrangian bird mesh (704 solid finite elements)

[Hugoniot Pressure = 300MPa, Stagnation Pressure = 30MPa]

Woven Glass Composite Model

The present paper describes the enhancements to the original model implementation into the explicit LLNL-DYNA3D of a damage mechanics based failure model [4]. The formulation is concerned primarily with in-plane failure in a woven glass composite, with *seven* damage variables introduced to model the observed fibre and matrix damage. Each damage variable has three fundamental relationships, which can be measured experimentally are:

- A stress threshold for damage to commence.
- The area under the stress-strain curve should be equal to the energy dissipated per unit volume.
- The power or energy dissipated per second must be bounded, e.g. fibre damage cannot grow faster than the crack velocity in the material.

Details of the original model formulation are presented in the open literature [4] hence only a summary and updates are presented in the current paper. The principal modifications relate to the inclusion of a new shear failure and compression failure laws, and a simplification of the matrix damage evolution law.

The damage mechanics formulation has been implemented within the existing shell element theory in LS-DYNA. The development of the damage model is hence restricted to plane stress assumptions. Each shell integration point through the thickness must represent each ply in the laminate. This allows damage information to be calculated and displayed on a ply-by-ply basis.

The damage components relating to the development of micro and macro cracks within the material, rather to any traditional plasticity concept. The composite damage model can predict tension and shear related failure modes:

- *Micro-matrix cracks* and fibre-matrix deterioration in the local weft (x) direction for each ply, d_{mx}.
- *Micro-matrix cracks* and fibre-matrix deterioration in the local warp (y) direction for each ply, d_{my}.
- *Fibre-matrix deterioration* due to in-plane (xy) shear for each ply, d_{mxy}.
- *Fibre fracture* in the local weft (x) direction for each ply, $d_{fx,t}$.
- *Fibre fracture* in the local warp (y) direction for each ply, $d_{fy,t}$.
- *Fibre compression* failure local weft (x) direction for each ply, $d_{fx,c}$.
- *Fibre compression* failure local weft (y) direction for each ply, $d_{fy,c}$.

The approach adopted is materially and geometrically non-linear in nature.

Evolution of Matrix Cracks

Matrix cracks are modelled using a micro-statistical, rate-dependent, internal state variable approach. This approach to modeling matrix cracks permits the degradation of the material elastic constants (matrix only) using the theory of mixtures.

Matrix crack damage evolution for a single ply in the local fabric x-direction was original given by:

$$\dot{d}_{mx} = (a_{10} + a_{11} d_{mx}) \left(\left(\frac{\sigma_x}{\sigma_{thres,mx}} \right)^2 - 1 \right) \quad (1)$$

To reduce the number of constants the growth period is assumed to consume substantially more energy than during the nucleation phase. Hence the current formulation uses the following equation;

$$\dot{d}_{mx} = \dot{d}_{mx,\max} \quad (2)$$

and $\sigma_{thres,mx}$ is the threshold for this type of damage to commence. A similar relationship exists for the y direction. Equations (1) and (2) control how fast damage can grow, since a lag will exist between the stress-time and damage-time curves a strain-rate affect can be implicitly modelled. Hence the greater the lag, the greater the enhancement to the stresses before degradation of the ply occurs.

Evolution of fibre fracture and fibre compression damage

Fibre fracture is modelled using a micro-statistical, rate-dependent, internal state variable approach. Fibre fracture and compression damage evolution in the local fabric x-direction is given by;

$$\dot{d}_{fx,i} = (a_{21} d_{mx} + a_{22} d_{fx,i}) \left(\left(\frac{\sigma_x}{\sigma_{thres,\,fx,i}} \right)^2 - 1 \right) \quad (3)$$

where 'i' can be either the fibre tensile failure or the compression failure and $\sigma_{thres,\,fx,i}$ is the threshold for damage to commence. A similar relationship exists for the y direction. A damage lag formulation is also employed which implicitly models the strain-rate effects observed, Equation (3). This accounts for the observed fibre pullout at the higher strain-rates, which requires additional energy to be dissipated. The formulation allows additional energy to be dissipated as both the strain to failure and stress to failure both increase as a function of strain-rate.

Elastic modulii and threshold stress

During unloading from a stationary condition the damage does not increase, unless the stress remains above the damage threshold. The values of the elastic constants are reduced by the damage already present in the material [5].

The mosaic model commonly used to model woven fabrics is adopted. Each fabric layer can be replaced by two uni-directional (UD) materials. A half thickness can be employed to represent the UD material. The first layer can be defined as:

$$E_{xx1} = 0.5(V_f E_f + V_m E_m)(1 - d_{fx}) \quad (4)$$

and the second layer as,

$$E_{xx2} = 0.5 \frac{E_m (1 - d_{mx}) E_f}{V_m E_f + V_f E_m (1 - d_{mx})} \quad (5)$$

The total Young's modulus in the local x-direction can be given by combining the above two equations,

$$E_{xx} = E_{xx1} + E_{xx2} \tag{6}$$

Similar equations exist for the local y-direction and for compression damage in which only the fibre modulus is degraded in Equations (4) and (5). The Poisson's ratios must be degraded in a similar manner to the Young's modulii to maintain the positive-definiteness of the material stress-strain law.

Energy dissipation

The engineering properties of the composite are reduced in proportion to the damage present in the material. In the process of crack growth, energy must be removed from the system. This can be achieved easily by reducing the stress threshold for each corresponding damage type, the stiffness (elastic modulii) is reduced concurrently.

Typically for matrix cracks, fibre fracture and compression failure in the local x-direction, the irreversible stress-rate can be defined as [6];

Matrix cracks: $$\dot{\sigma}_{x,ir,1} = f(\sigma_x, d_{mx}, \dot{d}_{mx}) = -\frac{\sigma \dot{d}_{mx}}{(1-d_{mx})}$$

Fibre fracture: $$\dot{\sigma}_{x,ir,2} = f(\sigma_x, d_{fx,t}, \dot{d}_{fx,t}) = -\frac{\sigma \dot{d}_{fx,t}}{(1-d_{fx,t})}$$

Fibre Compression: $$\dot{\sigma}_{x,ir,3} = f(\sigma_x, d_{fx,c}, \dot{d}_{fx,c}) = -\frac{\sigma \dot{d}_{fx,c}}{(1-d_{fx,c})}$$

which leads to Equation (7) for the 1-D case;

$$\dot{\sigma}_{xx} = E_{xx}\dot{\varepsilon}_{xx} + \dot{\sigma}_{x,ir,1} + \dot{\sigma}_{x,ir,2} + \dot{\sigma}_{x,ir,3} \tag{7}$$

The Young's modulus for a single layer or laminae is given by Equation (7), with the evolution of matrix damage given by Equation (1) and of fibre fracture given by Equation (3). Figure 5 shows the one-dimensional (warp or weft) stress-strain curve and the corresponding fibre fracture damage curve. The Young's modulus, given by Equation (7) is also presented in Figure 6.

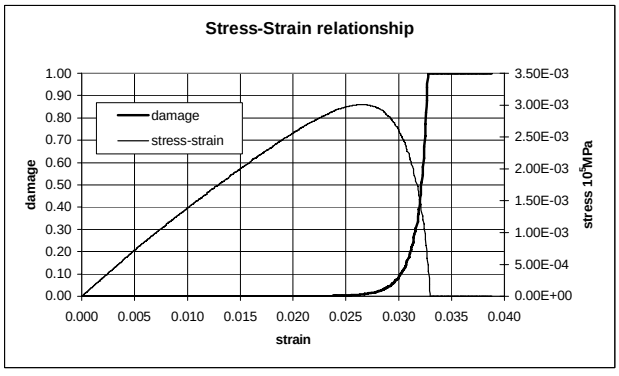

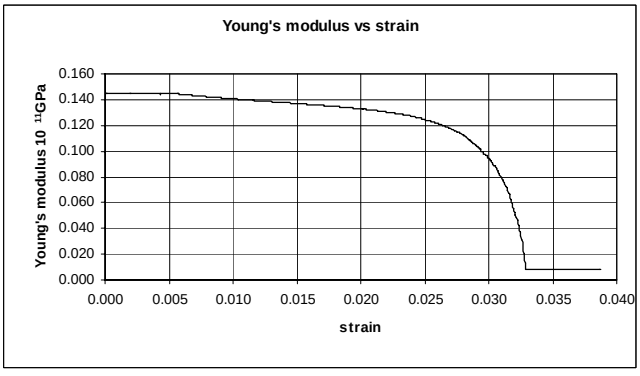

Figure 5. Direct stress-strain relationship for woven glass model (left)
Figure 6. Degradation of Young's Modulus against strain for model (right)

In-plane shear component and rate enhancement

A simple non-linear shear stress-strain behaviour is assumed for the in-plane shear response. The observed behaviour of woven glass (and carbon) fibre epoxies generally shows marked rate dependence in matrix-dominated modes, including shear related failure [6]. The shear stress-strain response is defined as:

$$G_{12}^{*} = (G_{12}^{0} - G_{2}) + G_{2}e^{-\lambda\gamma_{12}} \tag{8}$$

where G_{12}^{0} is the initial modulus, G_2 and λ are material constants, and γ_{12} the shear strain. The strain-rate enhancement is introduced with a unique scalar law based on the following equation:

$$\alpha = 1 + e^{\frac{\dot{\gamma}_{12}}{\chi}} \tag{9}$$

where χ is a constant, and $\dot{\gamma}_{12}$ is the shear strain-rate. The instantaneous shear modulus is then defined as:

$$G_{12} = \alpha G_{12}^{*} \tag{10}$$

Once initiation has occurred propagation of shear damage commences when the damage is equal to 1.0. Damage evolution follows the following relationship:

$$\Delta d_3 = \frac{\gamma_{\max,12}}{\gamma_{\max,12} - \gamma_{0,12}}\left[\frac{\gamma_{0,12}}{\gamma_{12}^{2}}\right]\Delta\gamma_{12} \tag{11}$$

where $\gamma_{0,12}$ is the shear strain when initiation commences, and $\gamma_{\max,12}$ is the ultimate shear strain when propagation of damage occurs. Unloading always follows the elastic unloading slope before damage commences, but it unloads with the damaged modulus when damage has initiated, Figure 7 illustrates this behaviour.

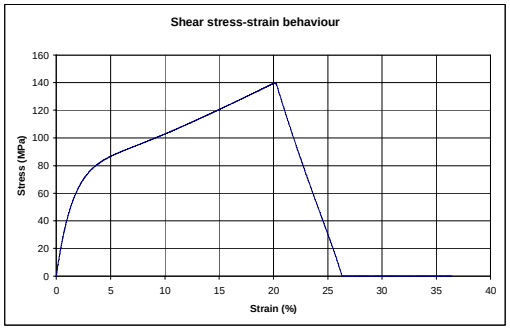

Figure 7. Shear stress-strain behaviour for woven glass

In-plane coupon tests

The material models described were used in a simulation of a tensile test. The matrix cracking and fibre fracture plots are shown in Figures 8 and 9, respectively. A displacement loading was applied using a dynamic relaxation approach within LS-DYNA. Element deletion occurs when fibre damage becomes equal to one, while matrix damage reaches saturation when damage is equal to one.

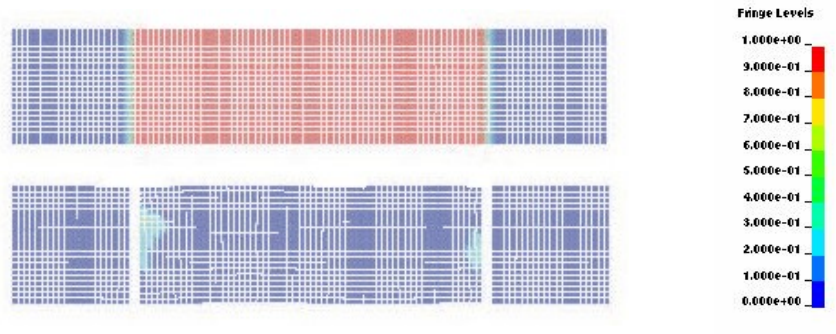

Figure 8. Coupon simulation for tensile specimen (matrix cracks, top)

Figure 9. Coupon simulation for tensile specimen (fibre failure, bottom)

The tensile-shear test (+/-45 degree laminate) was also simulated. The shear damage and matrix cracking plots are shown in Figures 10 and 11, respectively.

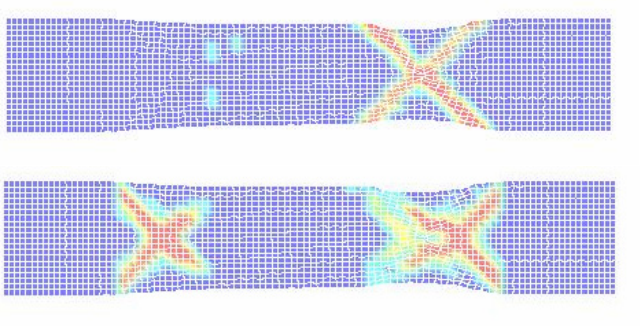

Figure 10. Coupon simulation for tensile-shear specimen (shear failure, top)

Figure 11. Coupon simulation for tensile-shear specimen (matrix cracks, bottom)

Bird Impact Modeling

The composite panels were modelled using thin shell elements. A user defined integration rule is used with equally spaced Gaussian points (each representing the number of plies in the panel) within the panel. Again the bird was modelled using an EOS validated during the rigid panel impact cases. The initial SPH distribution was generated automatically from a conventional solid FE mesh, with mass and particle density determined from those of the original solid element. Conventional penalty contact laws are used between particles and conventional finite elements, thus allowing a SPH bird model with a FE structural model.

Impact Simulations

The impact scenarios described in Table 1 are simulated using the modified version of LS-DYNA code incorporating the new damage model implemented as an additional material model option. The original Lagrangian FE models and simulations [2] are shown in Figures 12 to 14. In these cases SPH and bearing failure were not considered within the simulations.

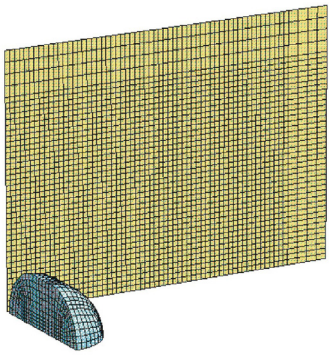

Figure 12. Composite panel FE shell mesh

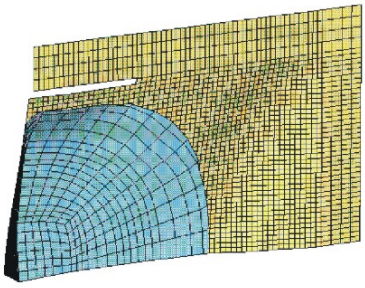

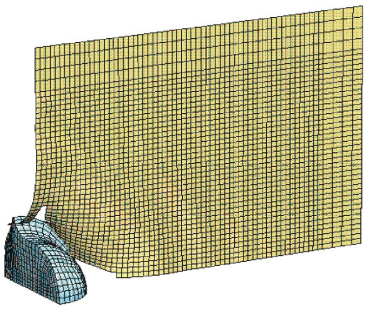

Figure 13. Impact case 147.5m/s – deformed shape (left)

Figure 14. Impact case 245m/s – deformed shape (right)

The experimental damage plots for the two cases in Table 1 are shown in Figure 15 and 16, respectively.

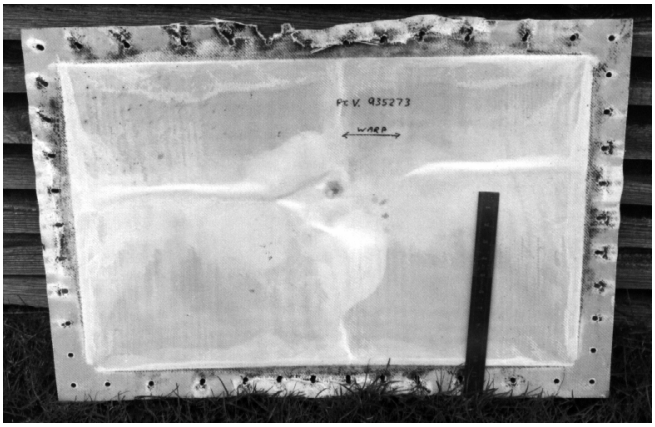

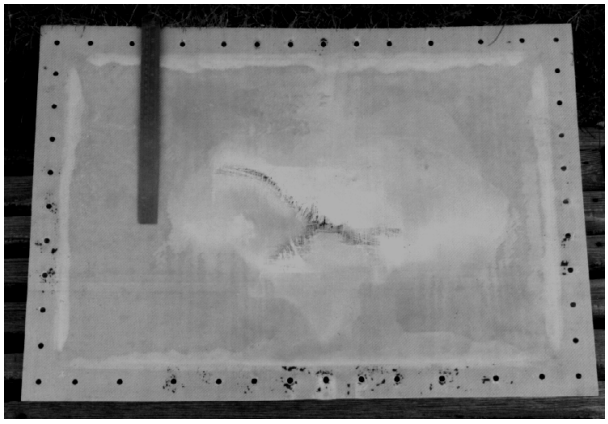

Figure 15. Impact case 147.5m/s – experimental deformed shape (left)

Figure 16. Impact case 245m/s – experimental deformed shape (right)

Materials Properties		
Warp Young's Modulus	E_x	13.5 GPa
Weft Young's Modulus	E_y	13.5 GPa
Young's Modulus of resin	E_z	3.5 GPa
Poisson Ratio	ν_{yx}	0.16
Poisson Ratio	ν_{zx}	0.069
Poisson Ratio	ν_{zy}	0.069
Shear Modulus	G_{xy}	3.26 GPa
In-plane Shear Strength		90 MPa
Warp Interlaminar Shear Strength		27.5 MPa
Weft Interlaminar Shear Strength		29.5 MPa
Density	ρ	1.38 g/cm^3
Warp Tensile strength*	x_t	250 MPa
Weft Tensile strength*	y_t	250 MPa
Warp Compressive Strength*	x_c	150 MPa
Weft Compressive Strength*	y_c	150 MPa
Volume Fraction for Fibres		26.5%
Volume Fraction for matrix		73.5%
Young's Modulus of resin Ec		3.5GPa
(* these properties were assumed for the simulations)		
Panels Two 6 ply (3mm thick) flat panels with a lay-up 0/90/0/90/0/90 and dimensions 750mmx500mm. Both panels are bolted via a clamping plate to distance of 50mm from the free panel edges. Normal incident impact of a 1kg bird projected using 6-inch gas gun.		
Panel (i)	287 knots impact case (global type failure)	No bird penetration, but extensive (between 40% - 50% of edges) bearing damage at support locations. Damage symmetrical in nature.
Panel (ii)	476 knots impact case (local type failure)	Bird penetrates the panel with extensive damage in the impact zone. The fracture surface had extensive fibre/filament pullout. Bearing damage substantially reduced, however, perforation outline not symmetrical.

Table 1 Summary of bird impact tests on woven glass panels [1]

Panel (i)

The overall agreement between the experimentally observed and numerically calculated damage is found to be very good. Extensive matrix cracks are predicted throughout the panel; however, no experimental data on the extent of matrix cracks is available for comparison. Figure 17 compares the numerical predictions with the experimental test for panel (i). The numerically calculated fibre fracture is predicted along the bolts holes. This matched the experimental observations indicate extensive bearing failure along similar regions. Bearing failure in this scenario is the preferred global failure mechanism and can occur before any composite fibre fracture at the point of contact, however, if a stress based failure model was used this would not be observed. Figure 18 illustrates the SPH bird flowing over the composite panel during the impact event, which is in surprising agreement with the original Lagrangian simulation.

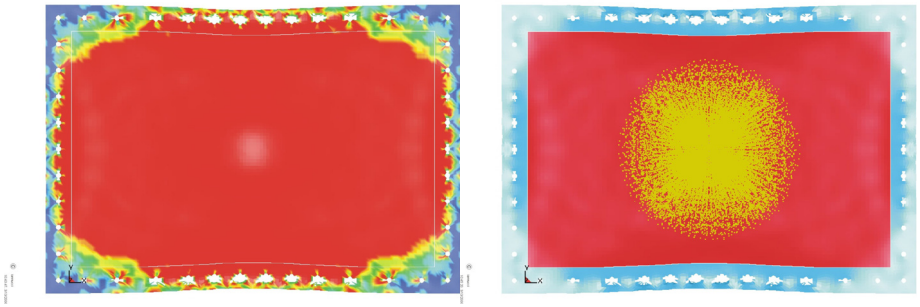

Figure 17. Composite impact case 147.5m/s – matrix cracks and fibre failure (left)

Figure 18. Composite impact case 147.5m/s – deformed shape with SPH particles (right)

Panel (ii)

Again, the overall agreement between the experimentally observed and numerically calculated damage is found to be very good. Figures 19 to 21 compares the numerical predictions with the experimental tests for panel (ii), respectively. The experimentally observed perforation is non-symmetrical in nature, whilst the numerical prediction is symmetrical in nature. This apparent discrepancy may be due to inhomogenities in both the experimental composite panel and bird. The bird may have impacted off-centre onto the composite panel or the fabrication procedure (hand lay-up) may not have generated all the warp or weft fibres in correct alignment.

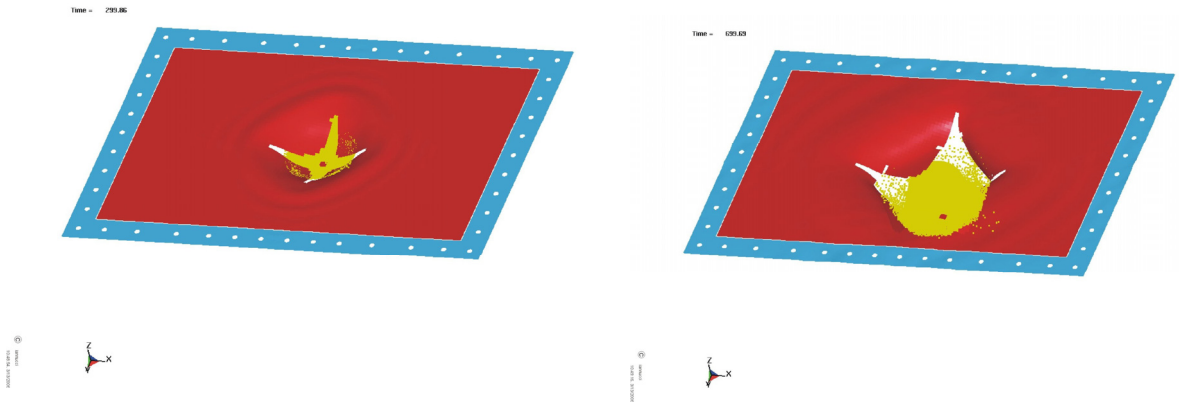

Figure 19. Composite impact case 245m/s – deformed shape time 300µsec (left)

Figure 20. Composite impact case 245m/s – deformed shape time 700µsec (right)

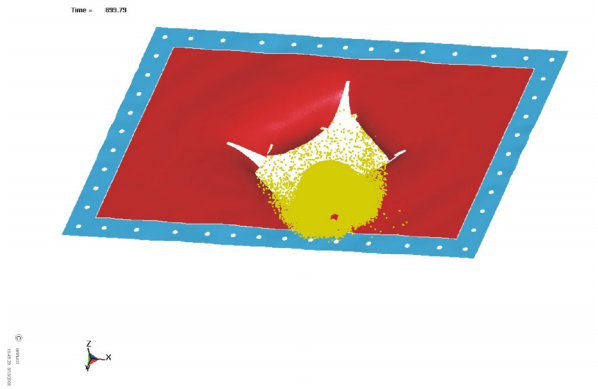

Figure 21. Impact case 245m/s – deformed shape time 900µsec

The kinetic energy of the bird is shown in Figure 22. Clearly the bird has considerable residual kinetic energy. The final deformed shape is shown in Figure 23.

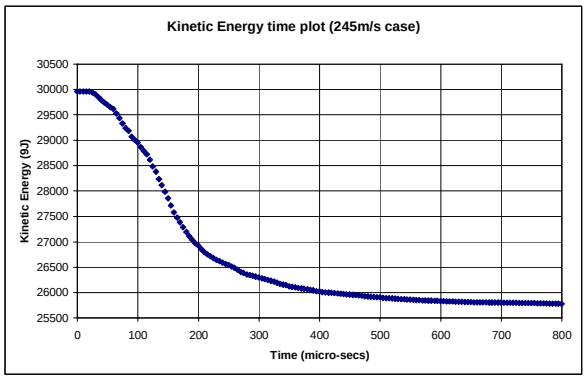

Figure 22. Kinetic Energy for composite bird impact case at 245m/s using SPH

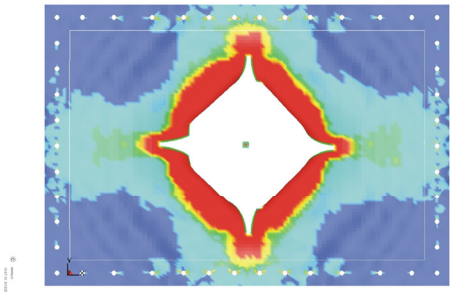

Figure 23. Composite impact case 245m/s – matrix and fibre damage

Conclusions

- In the present study the overall agreement between the experimentally observed and numerically calculated damage is found to be very good, considering the wide variability present in bird shape/properties and the extrapolation of dynamic properties.
- The use of a stress based failure model does not capture the global failure modes.
- The use of a *stress threshold* beyond which *energy dissipation* occurs with bounded *power dissipation* appears to yield reliable predictions for the behaviour of woven glass composites.
- The shell model implementation could be coupled to solid elements to realistic predict the delamination extent.
- The SPH bird modeling technique appears to be a robust approach for bird strike modeling.

References

1. Willows, M. L., Final report on the European Aerospace GARTEUR group on bird strike (AG23), QinetiQ, 2005.
2. Iannucci, L., Bird strike impact modeling, Foreign Object Impact and Energy Absorbing Structure, IMechE HQ, March 1998.
3. Barber, H. R. Taylor and Wilbeck, J. S., Bird Impact Forces and Pressures on Rigid and Compliant Targets, NASA AFFDL-TR-77-60, University of Dayton Research Institute Ohio, May 1978.
4. Iannucci L., Dechaene R., Willows M. and Degrieck J., A Failure Model for the analysis of thin woven composite structures under impact loadings, J. of Computers and Structures, Vol. 79, No 15, 2001, pp 785-799.
5. Iannucci L. and Arkenson, J., An energy based constitutive model for thin carbon composites, Composites Science and Technology, 2006, Vol. 66, Issue 7-8, pp 934-951.
6. Iannucci L., Progressive Failure Modeling of Woven Carbon Composite under impact, Int. J. of Impact, 2006, Vol. 32, No 6, pp 1013-1043.